Development of a Photocatalytic Wet Scrubbing Process for Gaseous Odor Treatment

Tong-xu Liu,[†,‡] Xiang-zhong Li,[*,†] and Fang-bai Li[‡]

Department of Civil and Structural Engineering, The Hong Kong Polytechnic University, Kowloon, Hong Kong, China, and Guangdong Key Laboratory of Agricultural Environment Pollution Integrated Control, Guangdong Institute of Eco-Environment and Soil Science, Guangzhou 510650, P.R. China

In this study, methyl mercaptan (CH_3SH) gas was used to prepare synthetic odorous gases, and a photocatalytic wet scrubbing process as a new approach was developed for treating such odorous gases. In this process, gaseous CH_3SH is first absorbed by the solution, and the dissolved CH_3SH/CH_3S^- is then adsorbed onto the solid surface of TiO_2 particles and oxidized under UV illumination in the aqueous phase. Experiments were conducted under different reaction conditions of CH_3SH loading, TiO_2 dosage, and pH. The reaction kinetics of CH_3SH reduction indicates that the pH of the reaction solution greatly influences the rate of CH_3SH absorption by the solution. At pH $<$ 11.5, CH_3SH absorption by the solution is the rate-determining step (RDS), whereas at pH $>$ 11.5, the photoreaction becomes the RDS in such a system. The experiments demonstrated that the efficiency of CH_3SH degradation determined by two methyl mercaptan sensors and the ratio of odor removal determined by olfactometry measurements can be well maintained at high levels of $>$95% for a CH_3SH loading of 10 g m^{-3} h^{-1}. The main intermediates and final products from CH_3SH degradation were identified by GC/MS and ion chromatography, and a pathway for CH_3SH degradation with three routes is proposed and discussed. Odor samples to simulate real foul gases were also prepared and treated with this new process. An electronic nose technique was applied to indentify the patterns of odor characteristics before and after treatment.

1. Introduction

Public concerns about odor problems remain at the top of air pollution complaints to regulators and government bodies in most urban cities such as Hong Kong.[1–3] Mercaptans, a type of sulfur-containing compound, are frequently identified in odor emissions from various sources such as sewage treatment works, refuse transfer stations, landfill sites, and other municipal waste management facilities. Among them, methyl mercaptan (CH_3SH) is a representative member with a very low odor threshold of around 0.4 ppb/v (parts per billion by volume).[4] Conventional technologies for gaseous odor treatment include (i) physical processes of condensation, adsorption such as activated carbon filters, and absorption such as by water scrubbers;[5,6] (ii) chemical processes such as wet chemical scrubbers, thermal oxidation such as catalytic incineration, catalytic oxidation, and ozonation such as UV + O_3 processes;[7–10] and (iii) biological processes of biofilters and bioscrubbers.[11] Among them, the scrubbing technique has proven to be one of the most effective and reliable processes for odor treatment. For example, in a wet chemical scrubber, the odorants can be quickly absorbed by liquid media such as water and then oxidized by some oxidizing reagents including chlorine, sodium hypochlorite, calcium hypochlorite, hydrogen peroxide, ozone, and potassium permanganate. In these processes, the absorbed odorants must be oxidized instantaneously to allow near-steady-state operation with continuous or periodical addition of the chemical reagents. However, it is difficult for either bioscrubbers or chemical scrubbers to discharge the treated gases with a sufficiently low odor concentration to comply with some stringent odor emission standards such as $<$100 OU_E m^{-3} (OU_E = European odor units), where odor sources are very close to their sensitive receivers without any buffer zones,[10,11] because the biomass and rudimental chemicals themselves are not odor-free substances.

Recently, many photocatalytic oxidation processes have been developed for air purification that are usually equipped with UV lamps and various solid photocatalyst films such as honeycomb-type or three-dimensional porous ceramic filters.[12–18] In such gas/solid systems, when foul air is passing through the reactor, the volatile substances in the gas can be transferred onto the solid catalyst film by adsorption/filtration and then degraded on the surface of the catalyst film under UV illumination through photocatalytic reactions.[19] However, the capacity for mass transfer and the rate of photocatalytic reactions are significantly restricted because of the limited surface area of solid catalysts,[20] as well as the accumulation on the catalyst surface of the residue of intermediates or final products after photoreaction, resulting in significant deactivation of the photocatalysts.[21,22] The wet scrubbing technique has proven to be efficient for mass transfer from the gaseous phase to the liquid phase by absorption,[23] and also photocatalysis processes using TiO_2 catalyst in its suspended form can achieve higher rates of photocatalytic reaction than those using TiO_2 films.[24] To combine both of these techniques, a photocatalytic wet scrubbing process can be developed as a new approach for gaseous odor treatment. This gas/liquid/solid system, compared to gas/solid systems, has several advantages in that rapid mass transfer is achieved because of the large contact area between the gas and liquid phases in a well-designed scrubber and the final products of photoreaction are easily dissolved into the solution to maintain the activity of the photocatalyst on its solid surface during operation. In addition, the treated gas has no residual odor because of no chemical addition. To the best of our knowledge, there is a lack of research about such a photocatalytic scrubbing process for gaseous odor treatment. Therefore, in this study, TiO_2 powder

* To whom correspondence should be addressed. Tel.: +852-27666016. Fax: +852-23346389. E-mail: cexzli@polyu.edu.hk.
† The Hong Kong Polytechnic University.
‡ Guangdong Institute of Eco-Environment and Soil Science.

10.1021/ie1000295

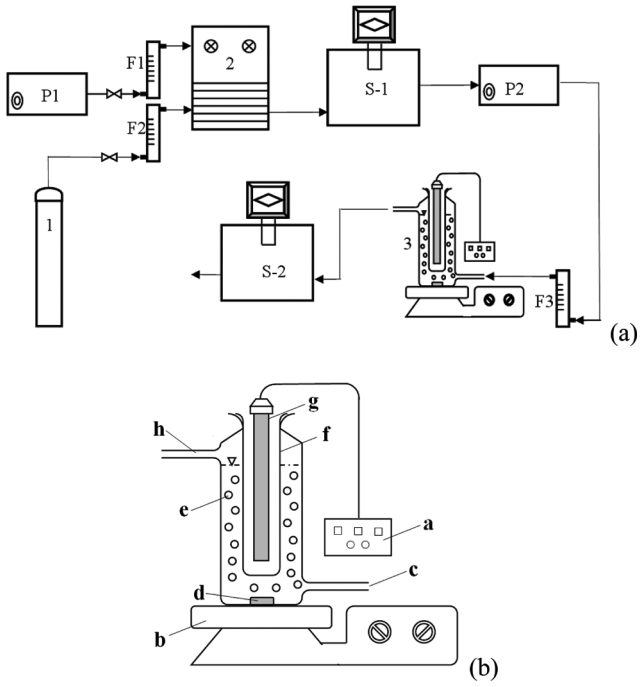

Figure 1. (a) Experimental setup of the photocatalytic wet scrubbing system: 1, CH_3SH gas cylinder; 2, mixing chamber; 3, photocatalytic scrubber; P1 and P2, air pumps; S1 and S2, CH_3SH sensors; F1−F3, gas flow meters. (b) Diagram of the photocatalytic scrubber: a, controller; b, stirring machine; c, gas inlet with an air diffuser; d, stirring bar; e, air bubbles; f, quartz jacket; g, light source; h, gas outlet.

was used as a photocatalyst, and a synthetic gas containing CH_3SH was prepared as a foul gas. The absorption and photocatalytic degradation of CH_3SH in a photocatalytic wet scrubbing system was investigated under different conditions including CH_3SH loading, TiO_2 dosage, and pH. At the same time, the reaction kinetics and the pathway of CH_3SH degradation were studied in detail.

2. Experimental Section

2.1. Materials. P-25 TiO_2 powder consisting of 80% anatase and 20% rutile was obtained from Degussa AG Company. Methyl mercaptan gas from a certified gas cylinder with a traceable concentration of 1990 ppm/v in air was supplied by BOC Gases and used as an odor source. CH_3SO_3H, H_2SO_4, and HNO_3 chemicals of analytical grade were obtained from Aldrich Chemical Co. and used without further purification. Deionzied and distilled water was used for the preparation of all aqueous solutions.

2.2. Equipment. As shown in Figure 1, CH_3SH gas from a cylinder was first purged into a mixing chamber made of Pyrex glass with an inner surface coated with a Teflon film to eliminate any adsorption, where it was mixed with odor-free air to dilute the CH_3SH gas to the required concentration. Two methyl mercaptan sensors were equipped to monitor the inlet and outlet CH_3SH concentrations. A cylindrical photoreactor containing an aqueous TiO_2 suspension was used as the photocatalytic scrubbing reactor, in which a medium-pressure mercury lamp (Philips, 8 W, 365 nm) with a light intensity of 1.28 mW cm^{-2} was positioned at its center. This cylindrical photoreactor was surrounded by a circulating water jacket to control the solution temperature at 23 ± 1 °C during the reaction and was covered with aluminum foil to avoid any indoor light irradiation.

2.3. Experimental Procedure. An aqueous TiO_2 suspension was placed in the photoreactor, which had an effective volume of 250 mL. The synthetic CH_3SH gas was continuously pumped into the TiO_2 suspension through an air diffuser at the bottom, and the suspension was magnetically stirred to ensure good contact between the dispersed gas bubbles and the solution for efficient absorption. To determine the amount of CH_3SH dissolved in the suspension, water samples were taken at given time intervals and immediately filtered through a 0.22-μm Millipore filter before analysis. Gas samples (about 60 L) were also collected using odor bags for olfactometry measurements to determine the odor concentrations.

2.4. Analytical Methods. Whereas gaseous CH_3SH concentrations were determined by the methyl mercaptan sensors (Detcon DM-100-CH_3SH) in the range of 0.1−100 ppm/v (±2%), the CH_3SH concentration dissolved in the solution was determined by the Ellman method as a widely used method to measure thiol groups in applied bioscience.[25] Some intermediate and final products from CH_3SH degradation in the aqueous phase, such as $CH_3SO_3^-$ and SO_4^{2-} ions, were analyzed by ion chromatography (IC) on a DIONEX ICS-90 instrument with an IC column (IonPac AS14A 4 × 250 mm). The odor concentration was determined using a forced-choice dynamic olfactometer (Olfactonate-n2) with a panel of human assessors in the range of $10-10^7$ OU_E m^{-3} according to European standard method EN13725. The patterns of odor characteristics were also examined using an electronic nose (E-Nose, FOX 3000) equipped with 18 different metal oxide sensors.

3. Results and Discussion

3.1. Absorption and Photodegradation. Three sets of experiments were first conducted at the pH values of 6.8, 10.9 and 12.5 to compare the CH_3SH removals in solution with and without TiO_2 catalyst, in which synthetic CH_3SH gas with an inlet concentration of ∼50 ppm/v was continuously introduced into the photoreactor at a gas flow rate of 600 mL min^{-1} under UV illumination for 45 min and the CH_3SH removal was determined by the difference between the CH_3SH concentrations in the inlet and outlet gases. The experimental results are presented in Figure 2a. It can be seen that, at pH 12.5, both CH_3SH removals in water-only solution and in TiO_2 suspension maintained high levels, because the dissolved CH_3SH concentration did not reach its saturated value in the solution after 45 min. At pH 10.9, the CH_3SH removal in the water-only solution gradually declined with reaction time with a half-life time of 12.6 min, whereas the CH_3SH removal in the TiO_2 suspension was maintained at a high level. At pH 6.8, the CH_3SH removals in water-only solution and in TiO_2 suspension demonstrated a pattern similar to that at pH 10.9, but the CH_3SH removal in the water-only solution declined much faster with a shorter half-life time of 4.5 min. These results show that the dissolved CH_3SH was successfully degraded in the TiO_2 suspension under UV illumination by 81%, 85%, and 99% at pH 6.8, 10.9, and 12.5, respectively.

In such a process, gaseous CH_3SH is first absorbed by the solution, and then the dissolved CH_3SH is adsorbed onto the surface of the solid TiO_2 particles and further photocatalytically oxidized under UV illumination in the aqueous phase. Hence, the concentration of accumulated CH_3SH in the suspension should eventually be stabilized at a certain level when the absorption rate is equivalent to the photoreaction rate. Figure 2b shows that the accumulated concentrations of CH_3SH in the water-only solution gradually increased with reaction time before reaching the saturated concentration. It can be seen that the saturated concentration of CH_3SH in the solution varied significantly from a high at pH 12.5 to a low at pH 6.8.

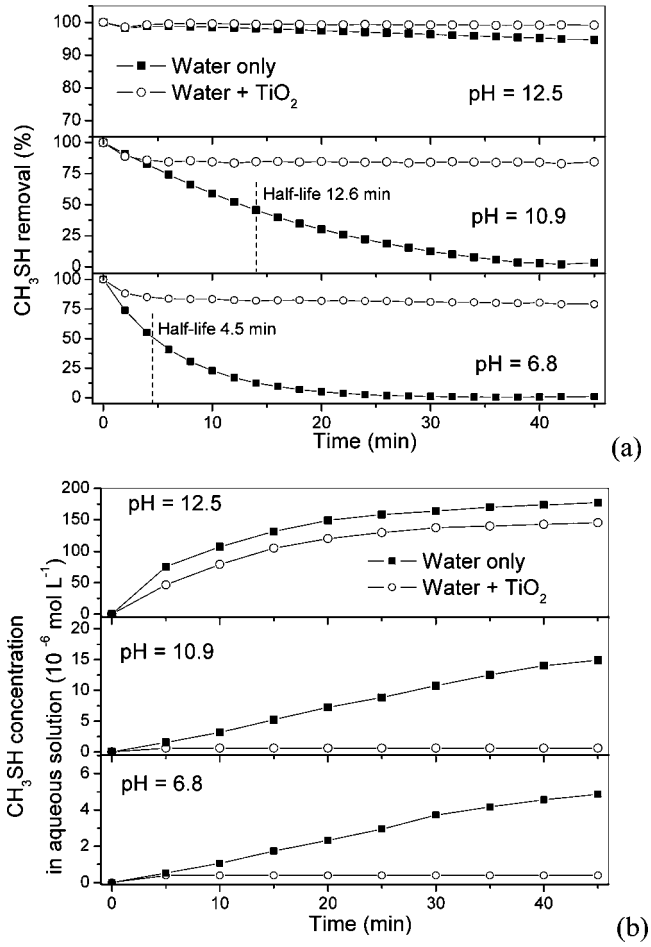

Figure 2. CH_3SH removal in the photocatalytic scrubber with and without TiO_2 catalyst under UV illumination at pH values of 6.8, 10.9, and 12.5, a TiO_2 solid content of 1 g L^{-1}, an inlet CH_3SH concentration ($[CH_3SH]_{inlet\text{-}gas}$) of ~50 ppm/v, and a gas flow rate of 600 mL min^{-1}. (b) Concentrations of dissolved CH_3SH in the aqueous solution during the photoreaction.

Furthermore, the results demonstrate that, although the two curves at pH 12.5 continuously increased in a similar pattern, the curves for the CH_3SH concentration in the TiO_2 suspensions remained at much lower levels than those in the water-only solutions at the lower pH values of 10.9 and 6.8. These results indicate that, at pH 12.5, the photoreaction rate is much lower than the absorption rate, whereas at lower pH, the absorption rate is lower than the photoreaction rate. Therefore, the rate-determining step (RDS) at high pH should be the photoreaction process, whereas the RDS at low pH should be the absorption process. Furthermore, it is well-known that CH_3SH can quickly dissociate as CH_3S^- in aqueous alkaline solution ($pK_a = 10.5$) as described by the equation[26]

$$CH_3SH + OH^- \overset{K_a}{\longleftrightarrow} CH_3S^- + H_2O \quad \text{(in alkaline solution)}$$

$$K_a = \frac{[CH_3S^-]}{[CH_3SH][OH^-]}$$

where K_a is the dissociation constant.

It can be seen that increasing the concentartion of OH^- ($[OH^-]$, i.e., increasing pH) will accelerate the dissociation of CH_3SH in aqueous solution.

3.2. Kinetic Study. To further study the kinetics of absorption and photodegradation of CH_3SH in the photocatalytic scrubbing system affected by solution pH, two sets of experiments for water absorption and photocatalytic reaction were conducted at different pH values. The first set of experiments for absorption was conducted in water-only solution in the dark but at different pH values for 45 min. The amounts of absorbed CH_3SH in the solution as a function of time for different initial pH values are shown in Figure S1a (Supporting Information). The second set of experiments on the photocatalytic degradation of CH_3SH through adsorption and photoreaction in TiO_2 suspension (TiO_2 = 1.0 g L^{-1}) containing a similar amount of CH_3SH under UV illumination was conducted as batch reactions, in which CH_3SNa was predissolved in the TiO_2 suspensions at different initial pH values and no CH_3SH gas was fed into the suspension during the photoreaction. The experimental results are shown in Figure S1b (Supporting Information). A first-order kinetic model was simply applied to fit the two sets of experimental data. k_{abs} is defined as the first-order rate constant of CH_3SH absorption by the solution

$$\text{absorption rate} = k_{abs}([CH_3SH]_{sat} - [CH_3SH])$$

and was determined from the data in Figure S1a (Supporting Information), whereas k_{rea} is defined as the first-order rate constant of the apparent photoreaction in aqueous solution

$$\text{photoreaction rate} = k_{rea}[CH_3SH]$$

and was determined from the data in Figure S1b (Supporting Information), where $[CH_3SH]_{sat}$ denotes the saturated concentration of dissolved CH_3SH in the aqueous phase and $[CH_3SH]$ denotes the actual concentration of dissolved CH_3SH in the aqueous phase. Because the concentration at all pH values reaches the saturation state after 1 h, the CH_3SH concentration in aqueous solution at 1 h (in Figure S1a, Supporting Information) was used as the value of $[CH_3SH]_{sat}$ for the calculation of the first-order rate constant of CH_3SH absorption. The values of k_{abs} and k_{rea} versus pH are plotted in Figure 3. It can be seen that k_{abs} increased dramatically with increasing pH, especially when the pH was higher than 11, but the k_{rea} changed only slightly at different pH values. The value of pH 11.5 can be identified as the point at which k_{abs} is equal to k_{rea}, which means that the RDS can be determined according to this critical pH condition. It can be concluded that the absorption process

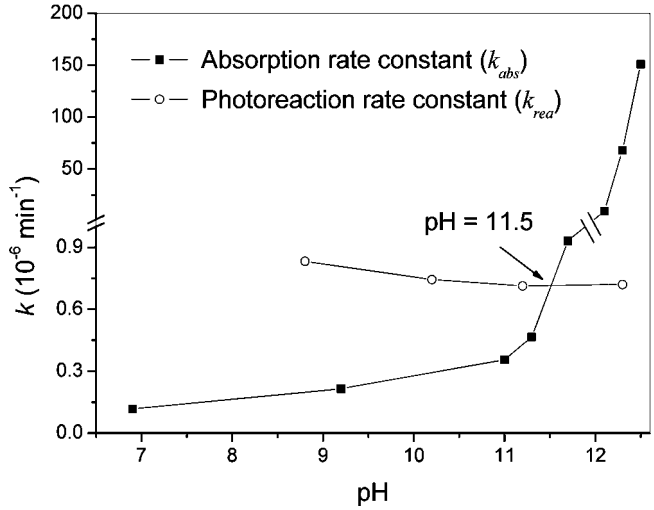

Figure 3. Dependence on pH of the kinetic rate constants for absorption in the dark (k_{abs}) and photodegradation of CH_3SH with TiO_2 under UV illumination (k_{rea}). (Conditions: TiO_2 dosage, 1 g L^{-1}; $[CH_3SH]_{inlet\text{-}gas}$, ~50 ppm/v; gas flow rate, 600 mL min^{-1}.)

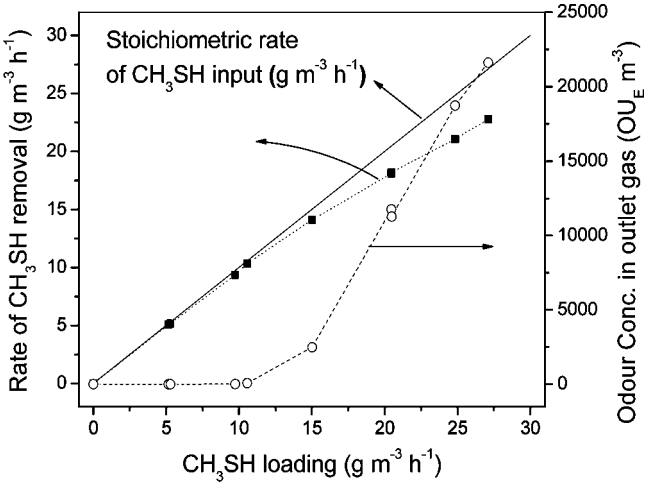

Figure 4. Dependence on CH_3SH loading ($[CH_3SH]_{inlet\text{-}gas}Q/V$) of the overall CH_3SH removal rate and odor concentration in the outlet gas (TiO_2 solid content, 1 g L^{-1}; $[CH_3SH]_{inlet\text{-}gas}$, ~50 ppm/v; gas flow rate, 600 mL min^{-1}; and pH, 11.5).

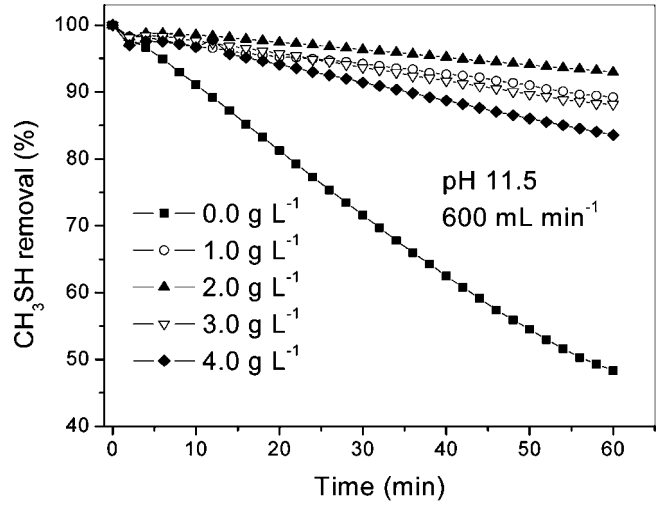

Figure 5. Dependence on TiO_2 dosage of the efficiency of CH_3SH removal ($[CH_3SH]_{inlet\text{-}gas}$, ~50 ppm/v; gas flow rate, 600 mL min^{-1}; and pH, 11.5).

(gaseous CH_3SH → dissolved CH_3SH/CH_3S^-) should be the RDS at pH values below 11.5, where $k_{abs} < k_{rea}$, whereas the photocatalytic reaction process (dissolved CH_3SH/CH_3S^- → products) becomes the RDS at pH values above 11.5, where $k_{rea} < k_{abs}$. Therefore, if the pH of an aqueous TiO_2 suspension were adjusted at around 11.5, the system could be operated under an optimized condition to achieve a balanced reaction rate between absorption and photoreaction under this experimental condition. However, such an optimized pH value could vary depending on several operating factors such as solution temperature, pressure, and power of UV lamp used in other reaction systems.

3.3. CH_3SH Loading. To study the effect of the CH_3SH loading on the CH_3SH removal, experiments were conducted at pH 11.5 with a TiO_2 dosage of 1.0 g L^{-1} but at different CH_3SH loadings. Whereas the first set of experiments was performed with a fixed gas flow rate of 600 mL min^{-1} but variable CH_3SH concentrations in the inlet gas, the second set of experiments was performed with a fixed CH_3SH concentration of ~50 ppm/v in the inlet gas but variable gas flow rates. During the experiments, the CH_3SH concentrations in the inlet and outlet gases were monitored by the sensors to evaluate the reaction rate and the efficiency of CH_3SH removal. The experimental results are shown in Figure S2 (Supporting Information) and further summarized in Figure 4. It can be seen that, when the CH_3SH loading was below 10 g m^{-3} h^{-1}, the rate of CH_3SH removal increased proportionally with increasing CH_3SH loading, and the efficiency of CH_3SH removal was maintained at a high level of >99%. When the CH_3SH loading was further increased, the increase in reaction rate was less than the increase in CH_3SH loading, and the efficiency of CH_3SH removal decreased rapidly. Furthermore, the odor concentration (OC) in the outlet gas determined by olfactometry measurements was very low (<10 OU_E m^{-3}) at a CH_3SH loading of 10 g m^{-3} h^{-1} or below, gradually increased in the range of 10−100 OU_E m^{-3} at CH_3SH loadings of 10−15 g m^{-3} h^{-1}, and quickly increased at CH_3SH loadings of above 15 g m^{-3} h^{-1} even though the efficiency of CH_3SH removal was still as high as 95%. It should be noted that the real odor impact from an odor control unit should be evaluated based on the odor emission rate (OU_E s^{-1}) calculated by the product of the OC (OU_E m^{-3}) and the outlet gas flow rate (m^3 s^{-1}).

3.4. TiO_2 Dosage. In Figure 5, the efficiency of CH_3SH removal increased as the TiO_2 dosage increased from 0 to 2.0 g L^{-1} and then decreased slightly with a further increase in TiO_2 dosage from 2.0 to 4.0 g L^{-1}. These results indicate that there is an optimum TiO_2 dosage at a certain intensity of UV illumination. Under the experimental conditions of this study, the TiO_2 dosage at 2.0 g L^{-1} achieved the best performance for CH_3SH degradation. It is well-known that the existence of a gradient distribution of light intensity within a photoreactor from high to low depending on the distance from the UV lamp should be the main reason to restrict the catalyst dosage to a certain level. Beyond such an optimum dosage, a gradient distribution of light intensity will achieve a great slope to drop sharply with the distance from the lamp because of serious light scattering resulting from the larger size or higher number of catalyst particles.[27] In other words, if the TiO_2 dosage is too high, the main photoreaction will occur only within a limited volume of reaction solution near the UV lamp. However, when a higher light intensity is applied, a higher dosage of TiO_2 should be used to achieve the maximum performance of the system.

3.5. CH_3SH Degradation Pathway. To study the pathway of CH_3SH degradation in such a photocatalytic scrubbing system, gaseous SO_2 as a possible product in the outlet gas was first examined using the a UV fluorescence SO_2 analyzer with a detection limit of 1 ppb/v. Three gas samples were collected from the outlet gas in the above experiments with CH_3SH loadings of 5.16, 10.57, and 20.46 g m^{-3} h^{-1}. However, all SO_2 concentrations were found to be <3 ppb/v, which means that SO_2 should not be a main final product in this process. Other possible intermediates and final products in aqueous solution were identified by gas chromatography/mass spectrometry (GC/MS) and IC analyses. Whereas some intermediates, namely, CH_3SSCH_3 (m/z = 94), $C_2H_6SO_2$ (m/z = 94), $C_2H_6S_2O_2$ (m/z = 126), and $C_2H_6S_2O_4$ (m/z = 158), were detected in the aqueous solution after 60 min of photoreaction by GC/MS, two main ionic products, $CH_3SO_3^-$ and SO_4^{2-}, and a minor product, $HCOO^-$, were determined by IC.

Based on the above identified components and relevant references,[28] a pathway for CH_3SH degradation through three routes of (i) C−S bond cleavage, (ii) polymerization, and (iii) S-atom oxidation is proposed as shown in Figure 6. The first process involves C−S bond scission induced by UV light irradiation to result in an increased amount of inorganic S at the TiO_2 surface. SO_4^{2-} then forms slowly according to the

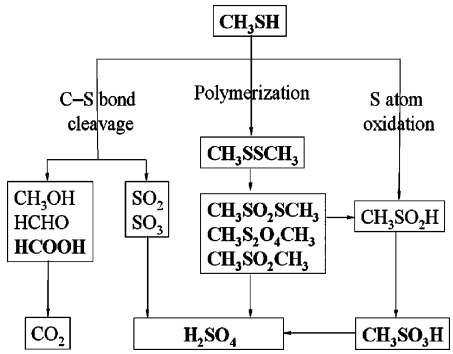

Figure 6. Proposed pathway of CH_3SH degradation in aqueous solution by photocatalysis.

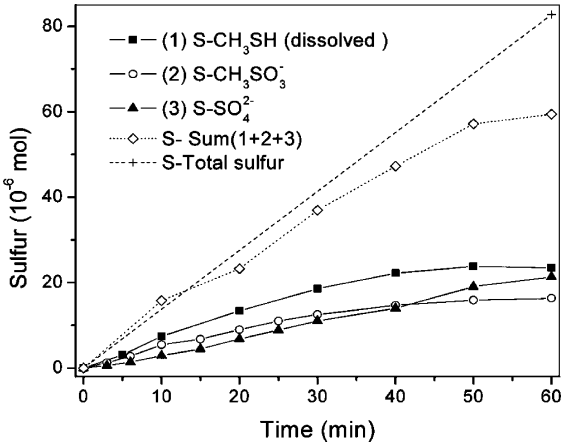

Figure 7. Mass balance of sulfur during the photocatalytic reaction ($[CH_3SH]_{inlet\text{-}gas}$, ~50 ppm/v; gas flow rate, 600 mL min^{-1}; and pH, 11.5).

observations of Lewis et al.[29] as a major product, along with some simple organic acids such as $HCOO^-$ as minor products. The second process was confirmed elsewhere[22] to be the major approach of CH_3SH degradation through polymerization and further oxidation reactions. The third process involves S−H bond dissociation and S-atom oxidation to SO_4^{2-} or other oxidized sulfur such as $CH_3SO_3^-$.

A mass balance of sulfur among the three sulfur-containing compounds of CH_3SH, $CH_3SO_3^-$, and SO_4^{2-} is summarized in Figure 7. The results show that, with increasing photoreaction time, the amounts of dissolved CH_3SH and $CH_3SO_3^-$ first increased and then eventually maintained a certain level, whereas the amount of SO_4^{2-} increased gradually all the time. Furthermore, it was calculated that the sum of the three amounts of dissolved CH_3SH, $CH_3SO_3^-$, and SO_4^{2-} was almost equivalent to the stoichiometric amount of CH_3SH input from the inlet gas during the first 20 min and then slightly less than the stoichiometric value because of the formation of more sulfur-containing intermediates at later stages of the reaction. These results confirm that $CH_3SO_3^-$ and SO_4^{2-} are the major intermediate and final product from the photocatalytic degradation of CH_3SH, whereas some other sulfur-containing intermediates are also formed as minor products.

Because the CH_3SH dissolved in aqueous solution is eventually converted to an acidic product of H_2SO_4, it is necessary to maintain the solution pH by continuously adding an alkaline chemical for the continuous operation of the process. As 1 mol of CH_3SH can form 1 mol of H_2SO_4, equivalent to 2 mol of NaOH consumption, this stoichiometic ratio can be applied as a makeup dosage for alkali addition in such a process.

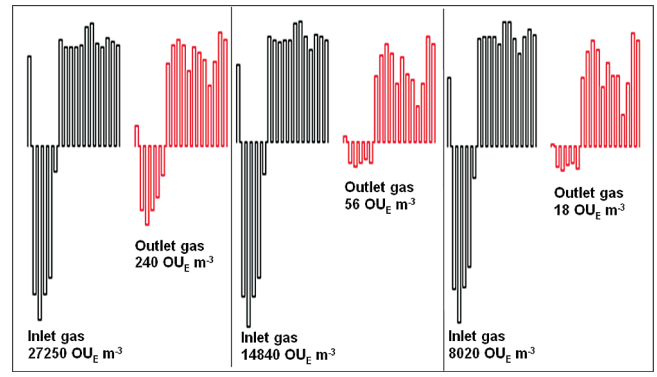

Figure 8. Results of olfactometry measurements for the odor concentration of real odorous gas samples and E-nose analysis for the fingerprints of real odorous gas samples.

Furthermore, a buildup of the SO_4^{2-} concentration in the solution will eventually affect the performance of the photocatalytic wet scrubbing system. Therefore, the solution containing TiO_2 catalyst needs to be replaced with clean water periodically, when the accumulated concentration of sulfate ions exceeds a certain level.

3.6. Potential Application for Gaseous Odor Treatment. Most odor emissions from municipal facilities have a common nature of being low in odor strength but high in foul gas volume. In this study, some real septic waste samples were collected from a local landfill site, and odorous gas samples were prepared by placing the waste sample in odor bags made of Nalophan material and then filling the bags with 60 L of odor-free nitrogen gas in our laboratory. After different retaining times, three odorous gas samples with different odor strengths were prepared and treated in the photocatalytic scrubbing system. The experiments were conducted under the operating conditions of pH 11.5, 1.0 g L^{-1} TiO_2 dosage, 600 mL min^{-1} inlet gas flow rate, and 1.28 mW cm^{-1} light intensity. The odor samples before and after treatment were analyzed by olfactometry to determine the odor reduction efficiency and also by E-nose to compare the patterns of odor characteristics before and after treatment. The analytical results are shown in Figure 8. It can be seen that the odor strengths of the three samples were greatly reduced from 27250, 14840, and 8020 OU_E m^{-3} to 240, 56, and 18 OU_E m^{-3}, respectively. The response of the E-nose to different samples after normalization is presented in Figure 8 as their fingerprints. It can be seen that the two sets of samples before and after treatment showed different patterns of fingerprints due to the photocatalytic reaction. By comparison with the standard patterns (Figure S3, Supporting Information) and specifications (Table S1, Supporting Information) of the sensors, it was found that the odor samples before treatment contained various components (ammonia, amines, hydrogen sulfide, mercaptans, etc.) detected by different sensors. For the treated odor samples, most sensors showed much weaker responses, and the patterns of E-nose response also changed significantly. Furthermore, the data obtained in E-nose measurements were further analyzed using the method of principle component analysis (PCA), and the two sets of samples (before and after treatment) were successfully classified into two separate groups by PCA according to the similarity of their odor characteristics with a discrimination index of 92 (Figure S4, Supporting Information). These results confirm the change in composition in the odor samples upon photocatalytic reaction.

4. Conclusions

A photocatalytic wet scrubbing process as a combination of the photocatalysis and scrubbing techniques was developed for treating odorous gases. Our experimental results confirmed that this process can effectively remove CH_3SH from synthetic odorous gas. The reaction kinetics of CH_3SH reduction showed that, at pH < 11.5, CH_3SH absorption by water is the rate-determining step (RDS), whereas at pH > 11.5, the photoreaction becomes the RDS in such a system. The experiments demonstrated that the efficiency of CH_3SH degradation and the ratio of odor removal could be well maintained at high levels of >95% when a CH_3SH loading of 10 g m^{-3} h^{-1} was used. The main intermediates and final products from CH_3SH degradation were identified as $CH_3SO_3^-$ and SO_4^{2-}, and a pathway for CH_3SH degradation with three routes was proposed. Real odor samples were also prepared and treated with this new process. The results of olfactometry and electronic nose measurements suggested that both the odor concentration and the odor patterns changed greatly after treatment by this process.

Acknowledgment

The authors thank the Hong Kong Government Research Grant Committee for financial support of this work (RGC no. PolyU 5232/08E).

Supporting Information Available: Dependence of CH_3SH dissolution and photoreaction on pH, dependence of CH_3SH removal on flow rate and inlet concentration of CH_3SH, standard pattern of sensors, grouping of odor samples by PCA, and specifications of sensors. This information is available free of charge via the Internet at http://pubs.acs.org/.

Literature Cited

(1) O'Neill, D.; Phillips, V. A review of the control of odour nuisance from livestock buildings: Part 3, Properties of the odorous substances which have been identified in livestock wastes or in the air around them. *J. Agric. Eng. Res.* **1992**, *53*, 23–50.

(2) Schiffman, S.; Bennett, J.; Raymer, J. Quantification of odors and odorants from swine operations in North Carolina. *Agric. Forest Meteorol.* **2001**, *108*, 213–240.

(3) Wright, D.; Eaton, D.; Nielsen, L.; Kuhrt, F.; Koziel, J.; Spinhirne, J.; Parker, D. Multidimensional gas chromatography−olfactometry for identification and prioritization of malodors from confined animal feeding operations. *J. Agric. Food. Chem.* **2005**, *53*, 8663–8672.

(4) Bashkova, S.; Bagreev, A.; Bandosz, T. J. Adsorption of methyl mercaptan on activated carbons. *Environ. Sci. Technol.* **2002**, *36*, 2777–2782.

(5) Bashkova, S.; Bagreev, A.; Bandosz, T. J. Adsorption/oxidation of CH_3SH on activated carbons containing nitrogen. *Langmuir* **2003**, *19*, 6115–6121.

(6) Sanchez, C.; Couvert, A.; Laplanche, A.; Renner, C. New compact scrubber for odour removal in wastewater treatment plants. *Water Sci. Technol.* **2006**, *54*, 45–52.

(7) Hancocka, F. E.; King, F.; Flavell, W. R.; Islam, M. S. Catalytically enhanced absorption of sulphur species from odorous air streams: A new technology for odour abatement. *Catal. Today* **1998**, *40*, 289–296.

(8) Couvert, A.; Charron, I.; Laplanche, A.; Renner, C.; Patria, L.; Requieme, B. Treatment of odorous sulphur compounds by chemical scrubbing with hydrogen peroxide−Application to a laboratory plant. *Chem. Eng. Sci.* **2006**, *61*, 7240–7248.

(9) Chu, Y. H.; Chiou, Y. Y.; Horng, K. H.; Tseng, T. K. Catalytic incineration of C_2H_5SH and its mixture with CH_3SH over a Pt/Al_2O_3 catalyst. *J. Environ. Eng.* **2001**, *127*, 438–442.

(10) Mills, B. Review of methods of odor control. *Filtr. Sep.* **1995**, *32*, 147–152.

(11) Burgess, J. E.; Parsons, S. A.; Stuets, R. M. Developments in odour control and waste gas treatment biotechnology. *Rev. Biotechnol. Adv.* **2001**, *19*, 35–63.

(12) Kato, S.; Hirano, Y.; Iwata, M.; Sano, T.; Takeuchi, K.; Matsuzawa, S. Photocatalytic degradation of gaseous sulfur compounds by silver-deposited titanium dioxide. *Appl. Catal. B* **2005**, *57*, 109–115.

(13) Yu, J. G.; Su, Y. R.; Cheng, B. Template-free fabrication and enhanced photocatalytic activity of hierarchical macro-/mesoporous titania. *Adv. Funct. Mater.* **2007**, *17*, 1984–1990.

(14) Li, Q.; Page, M. A.; Marinas, B. J.; Shang, J. K. Treatment of coliphage MS2 with palladium-modified nitrogen-doped titanium oxide photocatalyst illuminated by visible light. *Environ. Sci. Technol.* **2008**, *42*, 6148–6153.

(15) Liu, Y.; Li, Y.; Wang, Y. T.; Xie, L.; Zheng, J.; Li, X. G. Sonochemical synthesis and photocatalytic activity of meso- and macro-porous TiO_2 for oxidation of toluene. *J. Hazard. Mater.* **2008**, *150*, 153–157.

(16) Yu, J. G.; Wang, G. H.; Cheng, B.; Zhou, M. H. Effects of hydrothermal temperature and time on the photocatalytic activity and microstructures of bimodal mesoporous TiO_2 powders. *Appl. Catal. B* **2007**, *69*, 171–180.

(17) Liu, Z. Y.; Zhang, X. T.; Nishimoto, S.; Murakami, T.; Fujishima, A. Efficient photocatalytic degradation of gaseous acetaldehyde by highly ordered TiO_2 nanotube arrays. *Environ. Sci. Technol.* **2008**, *42*, 8547–8551.

(18) Fujishima, A.; Zhang, X. T.; Tryk, D. A. TiO_2 photocatalysis and related surface phenomena. *Surf. Sci. Rep.* **2008**, *63*, 515–582.

(19) Shiraishi, F.; Yamaguchi, S.; Ohbuchi, Y. A rapid treatment of formaldehyde in a highly tight room using a photocatalytic reactor combined with a continuous adsorption and desorption apparatus. *Chem. Eng. Sci.* **2003**, *58*, 929–934.

(20) Chang, H. T.; Wu, N. M.; Zhu, F. Q. A kinetic model for photocatalytic degradation of organic contaminants in a thin-film TiO_2 catalyst. *Water Res.* **2000**, *34*, 407–416.

(21) Vorontsov, V.; Kozlov, D. V.; Smirniotis, P. G.; Parmon, V. N. TiO_2 photocatalytic oxidation: II. Gas-phase processes. *Kinet. Catal.* **2005**, *46*, 422–436.

(22) Nishikawa, H.; Omamiuda, K. Photocatalytic activity of hydroxyapatite for methyl mercaptane. *J. Mol. Catal. A* **2002**, *179*, 193–200.

(23) Charron, A.; Couvert, A.; Lapanche, A.; Renner, C.; Patria, L.; Requieme, B. Treatment of odorous sulphur compounds by chemical scrubbing with hydrogen peroxide - Stabilisation of the scrubbing solution. *Environ. Sci. Technol.* **2006**, *40*, 7881–7885.

(24) Fernandez-Ibanez, P.; Blanco, J.; Malato, S.; de las Nieves, F. J. Application of the colloidal stability of TiO_2 particles for recovery and reuse in solar photocatalysis. *Water Res.* **2003**, *37*, 3180–3188.

(25) Riener, C. K.; Kada, G.; Gruber, H. J. Quick measurement of protein sulfhydryls with Ellman's reagent and with 4,4′-dithiodipyridine. *Anal. Bioanal. Chem.* **2002**, *373*, 266–276.

(26) Munro, A. P.; Williams, D. L. H. Reactivity of sulfur nucleophiles towards S-nitrosothiols. *J. Chem. Soc., Perkin Trans.* **2000**, *2*, 1794–1797.

(27) Yu, J. G.; Zhao, X. J.; Zhao, Q. N. Effect of surface structure on photocatalytic activity of TiO_2 thin films prepared by sol-gel method. *Thin Solid Films* **2000**, *379*, 7–14.

(28) Gonzalez-Garcia, N.; Ayllón, J. A.; Doménech, X.; Peral, J. TiO_2 deactivation during the gas-phase photocatalytic oxidation of dimethyl sulphide. *Appl. Catal. B* **2004**, *52*, 69–77.

(29) Lewis, M.; Tarlov, M. J.; Carron, K. Study of the photooxidation process of self-assembled alkanethiol monolayers. *J. Am. Chem. Soc.* **1995**, *117*, 9574–9575.

Received for review January 6, 2010
Revised manuscript received February 24, 2010
Accepted February 26, 2010

IE1000295